ORIGINAL RESEARCH

Seepage investigations of heterogeneous soils beneath some buildings using geophysical approaches: example from southwestern Nigeria

Adebayo Olayinka Salako[*] , Abayomi Gaius Osotuyi and Adekunle Abraham Adepelumi

*Correspondence:
salakoademi@gmail.com
Obafemi Awolowo University,
Ife, Osun, Nigeria

Abstract

Buildings along the flood plain of River Osun, southwest Nigeria, are usually thought of as been a safe haven for residence over the years. But in recent times with vast (increasing) population and growing urbanization, some of the buildings currently experience structural damages not related to constructional designs but rather ground conditions around building foundations. The ground conditions (seepages in this case) and how it influences properties of soils (water moisture, permeability etc.) to support the foundation of buildings. This paper attempts to map out seepages in heterogeneous soils around buildings in Erinle, southwest Nigeria where building cracks probably as a result of water seepages from subsurface through fissures and fractures where noticed. These cracks are a probable manifestation of a weakened foundation that could overtime result to a collapse, hence the need to investigate seepage prone zones. To achieve this, electrical resistivity (ER) and Electromagnetic Ground Penetrating Radar (EM-GPR) surveys were made along affected buildings to map out possible causes of deterioration. Geo-sections (analyzed ER data) shows high resistivity layer (topsoil) underlain by low resistivity layer (weathered basement) confirmed by planer reflections (topsoil) and fairly smooth to smooth reflections (weathered basement) in Radargrams (analyzed GPR data). An integration of the geo-section and radargram produced from ER and GPR data shows that buildings along traverses 1, 2, 3 and 5 is most prone to seepages especially as it exhibits very low anomalously resistivity values (< 25 Ωm) but this is not the case for buildings along traverses 4, 6, 7 and 8.

Keywords: Seepages, Heterogeneous soils, Ground Penetrating Radar (GPR), Electrical resistivity (ER), Radargrams, Geo-sections

Introduction

Soils, the starting geological material of rocks are mostly heterogeneous by nature, this been due to the varying proportions in which their components combined both physically, chemically and biologically. As such the different components that make these soils would have different degrees of variability [15] resulting in deteriorations along planes of weakness (fractures or fissures) and serving as routes or pathways for water seeps. Seepages especially those of groundwater origin overtime results to erosion, that weaken

the foundation of buildings. According to McLean and Gribble [16], anomalous seepages are sometimes found occurring through permeable soils and rock aquifers controlled by their structure/bedrock topography and faults/master joints. The use of the drilling technique, for groundwater investigation and mapping would have been suitable for mapping seepages except for its limitations in the areas of time consumption, data coverage and expense thus preempting the need to adapt other proficient techniques to compensate for these limitations.
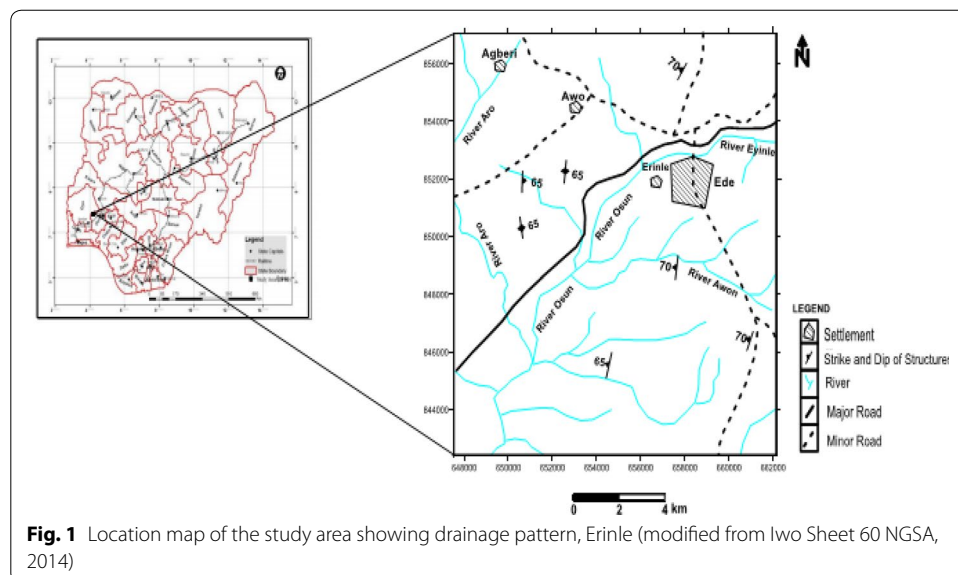
In recent years, geophysical techniques such as electrical resistivity, seismic, gravity, magnetic, ground penetration radar, etc. has been increasingly adopted in many projects related to both engineering and environment due to their ability to be implemented less expensively and more quickly in covering large areas thoroughly [4, 9, 13, 14, 23]. The application of electrical resistivity (ER) has proved a most successfully tool in groundwater resource mapping as groundwater movement and its existence are largely localized and difficult to predict [1, 11]. The use of ER has also proven significantly sensitive to variations in resistivity of earth materials with particular reference to water occurrences, and engineering site characterization [21, 31] given more precise results due to the improved development in electronic technology.

Ground Penetrating Radar (GPR) is a powerful non-destructive tool that is used for many diverse applications in fields such as engineering, geophysics and even medicine. Examples include: infrastructure assessment of bridges, roads, and railways; locating buried utilities; ice profiling and glaciology; groundwater and soil contaminant mapping; landmine and unexploded ordnance (UXO) recognition; and detection of breast cancer tumours [12, 30]. GPR has the potential to non-invasively investigate geologic heterogeneity at high resolution over large volumes of the subsurface. GPR image possesses important parameters that help delineate regions of similar subsurface characteristics [7]. The EM velocity field is crucial in many processing steps, such as, for example, depth conversion and imaging, and provide essential information to characterize subsurface materials. Compared to other methods for the measurement of soil water content, GPR as a non-invasive geophysical technique, can measure a larger area easily and quickly with a high spatial and temporal resolution [6, 17]. Ground Penetrating Radar technique (GPR) like its counterpart electrical resistivity (ER) has been used by several authors like [20] to carry out investigations of the shallow subsurface like the conductivity mapping of saline water; in bedrock profiling, fracture mapping, and in sedimentology [5, 18]; in lossless homogeneous and lossy heterogeneous environments [29]. The effects of vegetation, water puddles, rough surface, and complex soils have been examined and cases shown for which GPR—using the specific modeled antennas [8]. Targets and soil characteristics have effect on back-scattered radar signal. To evaluate these changes in a quantitative way a similarity measure was performed (via the correlation coefficient) between time domain signatures [10]. Physical and geometrical parameters that influence target radar response are shown below [27]; as (i). Soil EM constitutive parameters μ_r, ε_r (ii). Target depth and orientation with respect to the soil surface.

Thus, the use of GPR is necessary in this investigation as it seeks to measure the propagation of velocity and reflection amplitude of the electromagnetic waves across the area to be surveyed thus making a powerful technique for imaging lateral and vertical variations of the subsurface. These variations could include variations in soil type, depth mapping and possible subsurface cavities and voids. Prevention of damages due to pavement pumping and the presence of clay in pavement structural layers under dry conditions was predicted using GPR technique by [26]. The method has been tested in sub-grade and sub-base soils using different GPR systems to evaluate as it performs as the data were post-processed in the frequency domain. The results of two surveys (ER and GPR) when integrated is expected to characterize the heterogeneous soils (varying subsurface layers) sufficiently enough to map out seepage zones and reveal reasons for the cracks found on walls of the buildings.

Site description

The investigated site (Adeje Estate) is located along the western bank of River Osun in one of the moderately populated areas of Erinle (Fig. 1). The site under consideration is located along latitudes N7°45′1″ and N7°45′3″, and Longitudes E4°25′49″ and E4°25′52″ (Fig. 2) and made up of six buildings with more than half of it been occupied by the buildings while the remaining fractions had been used as parking lots. The buildings used for residential purpose mainly are accessible through footpaths and the Ede–Oshogbo road with the eastern and western sides of the site facing two moderately low-traffic streets. Four out of the six buildings situated in the northwestern direction of the site along traverses 1, 2, 3 and 5 and represented as G1, G2, G3 and G5 show signs of structural weakness through with groundwater seeps out (Figs. 3, 4) while the remaining two shows no signs of such. This structural problem (wall cracks) experienced in the site is probably of geological origin as site is not close to any mining activities, railway stations/tracks or any other activity that would have resulted in wall cracks and water seeps as shown in some buildings.
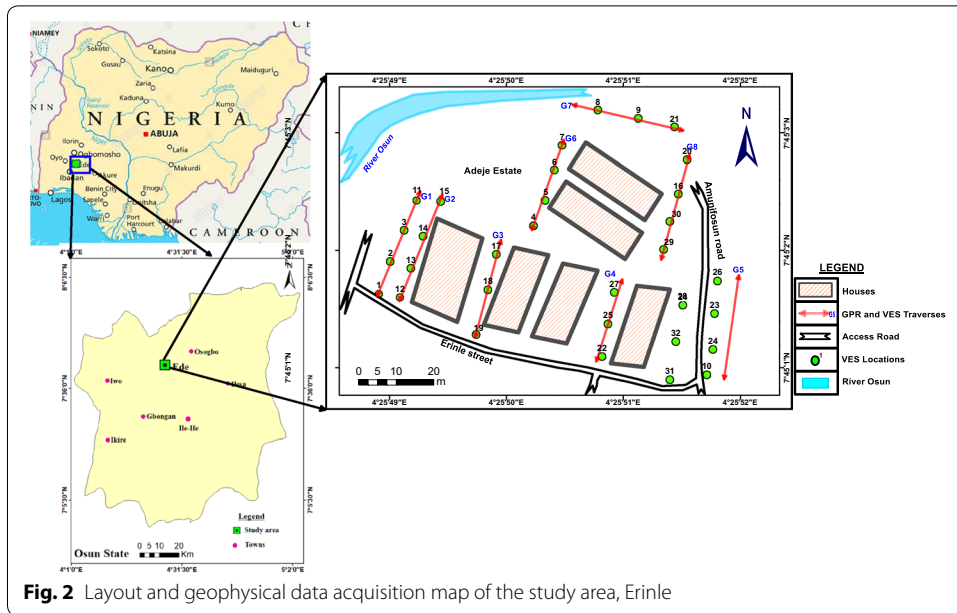

Fig. 1 Location map of the study area showing drainage pattern, Erinle (modified from Iwo Sheet 60 NGSA, 2014)

Salako *et al. Geo-Engineering*   (2019) 10:11

Page 4 of 20

Fig. 2 Layout and geophysical data acquisition map of the study area, Erinle

Fig. 3 Picture of seepage through building floor

Fig. 4 Picture of seepage through cracks on walls

Geological setting and structural background

According to [19, 22, 25], the study area is being underlain by rocks of the Migmatite–Gneiss–Quartzite Complex forming one of the six lithological groups making up the Nigeria basement complex, particularly it falls within the Precambrian Basement Complex of Nigeria of SW Nigeria. A close examination of the study area shows that it is been characterized by three major rock units; from the oldest to the youngest in terms of geological age namely; Undifferentiated Migmatite, Charnokitic Meta-intrusives and lastly Pegmatites (Fig. 5). Structurally, the subsurface of the investigated site probably have been subjected to some form of deformational episodes characterized by geological structures such as fractures, fissures, faults thus given the fault system a NE–SW trend. Groundwater finds its way to the surface through these fissures, fractures and faults which gradually results to a weakening of building foundations. These weakening probably is what translates to building cracks as noticed by some buildings resulting in a geometrically increase of water seeps through walls especially during the raining season which poses a lot of risk to residents.

Geophysical data acquisition and processing

Ground Penetrating Radar (GPR) survey

Ground Penetrating Radar (GPR) survey uses contrasts in dielectric permittivity between subsoil to characterize the subsurface. Its operation is based on transmission of electromagnetic pulses (i.e. radio waves) at high frequency from a transmitting antenna to the subsurface to probe the lossy dielectric material, and recording of the reflected pulse responses from the interfaces and objects buried below within the subsurface. Variations between subsoil results in reflections in as witness in GPR processed data; the greater the difference in dielectric permittivity (variation in textural, lithology and porosity of subsoil), the greater the coefficient of reflectivity translating to variations in
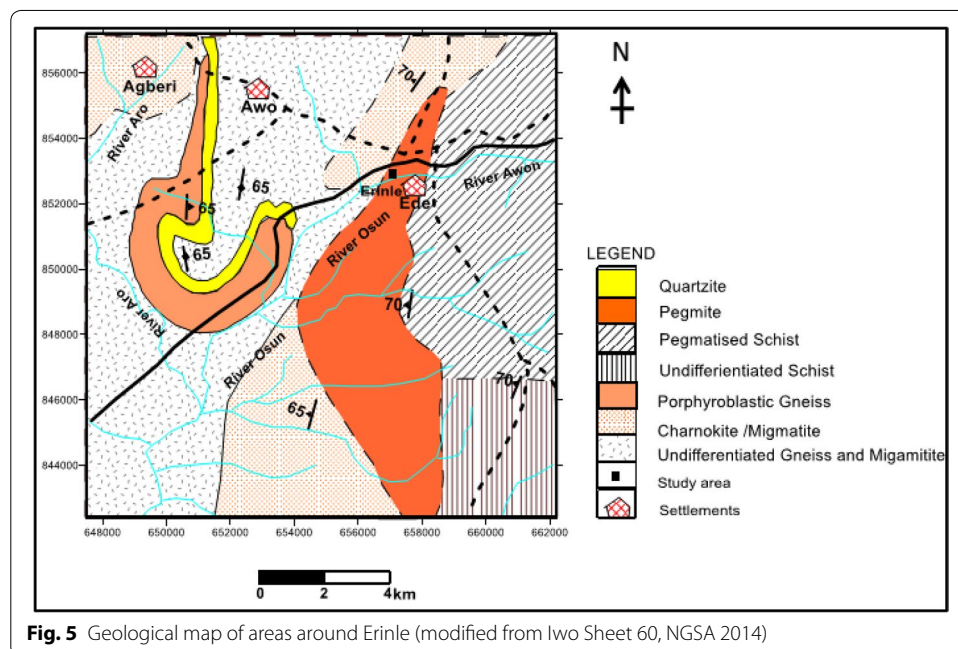

Fig. 5 Geological map of areas around Erinle (modified from Iwo Sheet 60, NGSA 2014)

GPR reflection patterns [3]. A total of about 8 (eight) GPR profiles were acquired along investigated site with varying lengths ranging between 80 and 100 m. The GPR data obtained were acquired using the SIR 2000 System by GSSI equipped with a 200 MHz shielded mono-static antenna oriented in a broadside survey direction. The data were acquired in a continuous mode with a time sampling interval of 1024 and a time interval of 300 ns. Optimum data quality was aimed at when designing and conducting the survey by putting into consideration the factors that could degrade the data such as uneven ground surface, system noise, overhead reflections from power lines trees, and external electromagnetic noise from radio transmitters. Estimated velocities electromagnetic waves through some of the materials encountered in the study area as gotten from literatures are shown in table below in Table 1.

The GPR data were then processed using RADPROfWin 3.4 GPR software to remove noise and enhance imbedded subsurface features signals. To facilitate this, several other processing steps were applied including:

a. Static correction for the ground zero level
b. Background removal to facilitate the recognition of imbedded intra-structure
c. Band-pass 2D filter to remove noise and get clear sections
d. Application of Automatic Gain Control (AGC) and Normal Moveout (NMO) to help in subsurface characterization

Electrical resistivity (ER) survey

The use of electrical resistivity (ER) method for electrical resistivity survey seems to be one of the common geophysical techniques applied in shallow subsurface investigations due to ease and economical usage in terms of field logistics. The survey was applied using Vertical Electrical Sounding (VES) technique which measures lateral and vertical changes in subsurface resistivity. Data acquisition for the survey was carried out along eight traverses, adopted using Schlumberger configuration of 80 m spread along a half-current electrode spacing (AB/2) thus giving a total of thirty-two (32) VES points. The

Table 1 GPR velocity table and analysis of velocity, dielectric constants, attenuation, and conductivity values for materials from various sources

Material	Dielectric constant K	Conductivity (mS/m)	GPR velocity (m/ns)	Attenuation (dB/m)
Air	1	0	0.3	
Asphalt	3	0.001–0.01	0.14	
Concrete (dry)	7	0.001–0.01		
Concrete (wet)			0.09	
Clays	5–40	2–1000	0.06	1–300
Granite	4–6	0.01–1	0.13	0.01–1
Granite (dry)	5	0.00001	0.134	
Granite (wet)	7	110.12	0.40	
Mixed soil components saturated	5–15		0.08–0.13	
Rock (dry)	5	0.00001		

Salako *et al. Geo-Engineering*　(2019) 10:11

Page 7 of 20

Resistivity data obtained at the various stations were then plotted against the half-current electrode spacing (AB/2) and processed using the WinRESIST software developed by [28]. Processed results were stacked together to develop 2D geoelectric section of the subsurface to better characterize the subsurface. Processed results were stacked together to develop 2D geoelectric section of the subsurface to better characterize the subsurface thus providing engineers with detailed information on subsurface ground conditions.

Data interpretation

We attempt here to interpret the various data as obtained from Ground Penetrating Radar (GPR) and Vertical Electrical Sounding (VES). The results obtained from the processed GPR data are interpreted in terms of the radar facies and the VES data are represented as Geoelectric Sections, Isopach and Isoresistivity Maps. These have profiles running north–south so as to capture subsurface features and lithology across regional and local geologic strike so as to ensure maximum energies (as shown by the isopach and isoresistivity maps), except along profile 7 running east–west.

Results and discussions

Geoelectric sections, isopach maps and isoresistivity maps

Due to the objectives and aims of this research, data obtained from VES were carefully planned and cited to produce a 2D Geo-section that mirrors the events of the underlying subsurface/subsoil. The geo-section as illustrated by Figs. 6, 7, 8 and 9 shows three distinct layers (topsoil, weathered layer and basement). Our interest here, however is the weathered layer made up weathered basement material and clay rich soils which varies both laterally and vertically across the investigated area with relative thickness of about 3–12 m and low resistivity values of 19–282 Ωm especially in Fig. 6. Where resistivity value is as low as 19 Ωm. Buildings along traverses 1, 2, 3 and 5 are rooted within anomalously low resistivity (<65 Ωm) with high relative thickness; the anomalously low resistivity (Fig. 7) probably suggests or reflects the presence of clay with intercalations of sands (within weathered layer) or higher water content. The gradual expansion and contraction of clay here gradually weakens the foundation which probably reflects as cracks on the building walls. Also the high water content exhibited by the weathered layer makes these traverses more susceptible to seepages as water from below finds its way to the surface through cracks already created by the gradual expansion and contraction of clay within the weathered layer. This is however not the case with houses situated along traverses 4, 6, 7 and 8 (Figs. 7, 9).

Isopach maps drawn generally give spatial distribution of areas with equal thickness across the area of study. Based on this, relative thicknesses of topsoil, weathered layer and the overburden (topsoil + weathered layer) across all eight traverses were collated and carefully plotted to produce varying Isopach maps (Figs. 10, 11, 12).

In Fig. 10, the Isopach map of the topsoil gives a description of the spatial distribution of areas with equal thicknesses across the study area. Most part of the site is of relatively thin overburden thickness of < 5 m except the extreme south–south east (SSE) with about > 9 to 15 m thickness. Figure 11, reveals from the Isopach map of the weathered layer that this layer thins out from the central area to the northwest (NW) with the thickness ranging from 12 to 5 m. Thick weathered layer are observed on the northeast

Salako *et al. Geo-Engineering* (2019) 10:11

Page 8 of 20

Fig. 6 Geoelectric sections along traverse 1 and 2
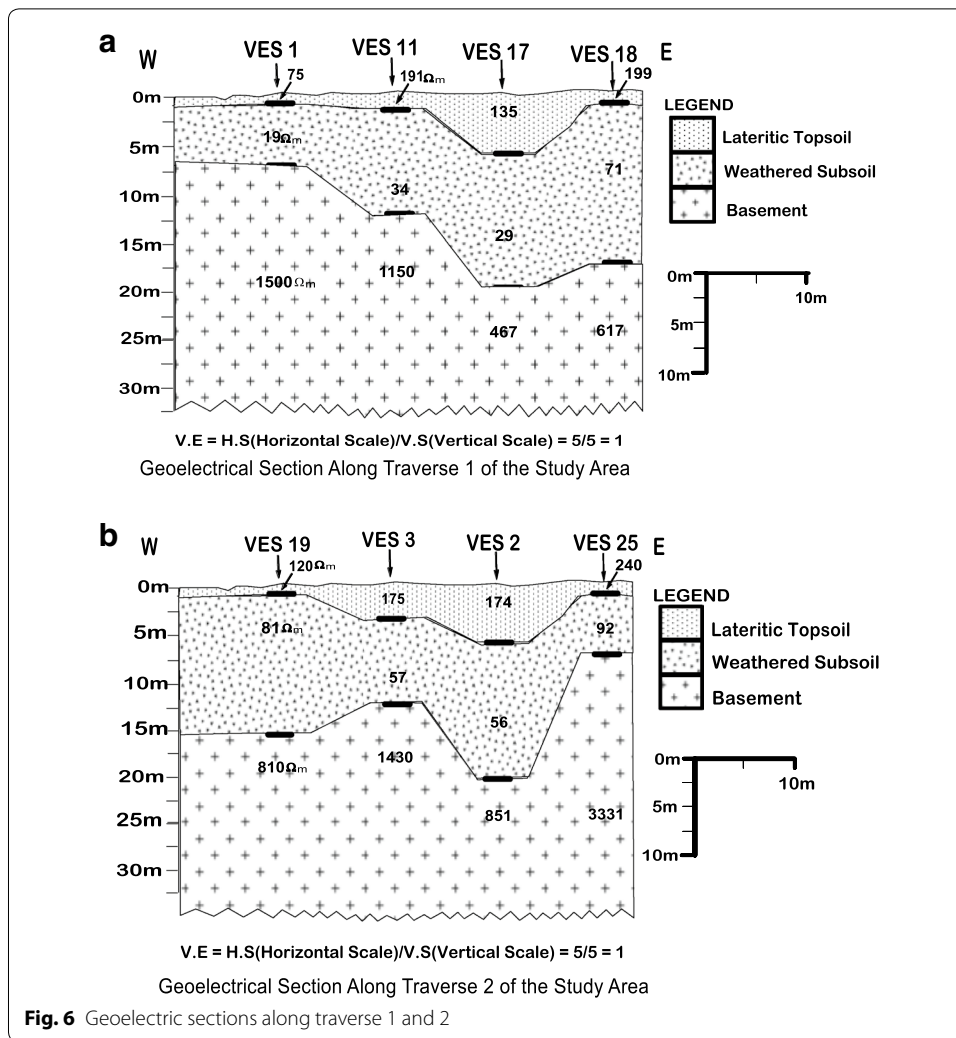
(NE) flank down toward the SE, S and SW ranging from 22 to 14 m. The thickness is sufficiently considerable for groundwater accumulation in the weathered layer.

The isopach map in Fig. 12 reveals that Overburden thins from the central area to the northwest (NW) part of the study area ranging from about 14 to 8 m. also, thick Overburden are revealed on the northeast (NE) flank toward the southeast (SE) ranging between 17 and 27 m and fairly thick overburden at the centre towards the South ranging between 15 and 22 m.

The depth to basement map and wireframe reveals the depth to basement across the area range from 9 to 27 m (Figs. 12, 13 and 14). Areas with thin overburden coincides with Basement topographic high and areas with thick overburden coincide with basement topography low (Figs. 12, 13 and 14). Areas with thick overburden coincide with Basement depression. These zones may serve as depo-centers for groundwater accumulation and build-up. These zones also coincide with the low resistivity region characterized as clayey. The zones with weathered layer resistivity < 400 Ωm, signifies clayey sand/sandy clay known for poor hydraulic conductivity but high water capillarity.

Fig. 7 Geoelectric sections along traverse 3 and 5
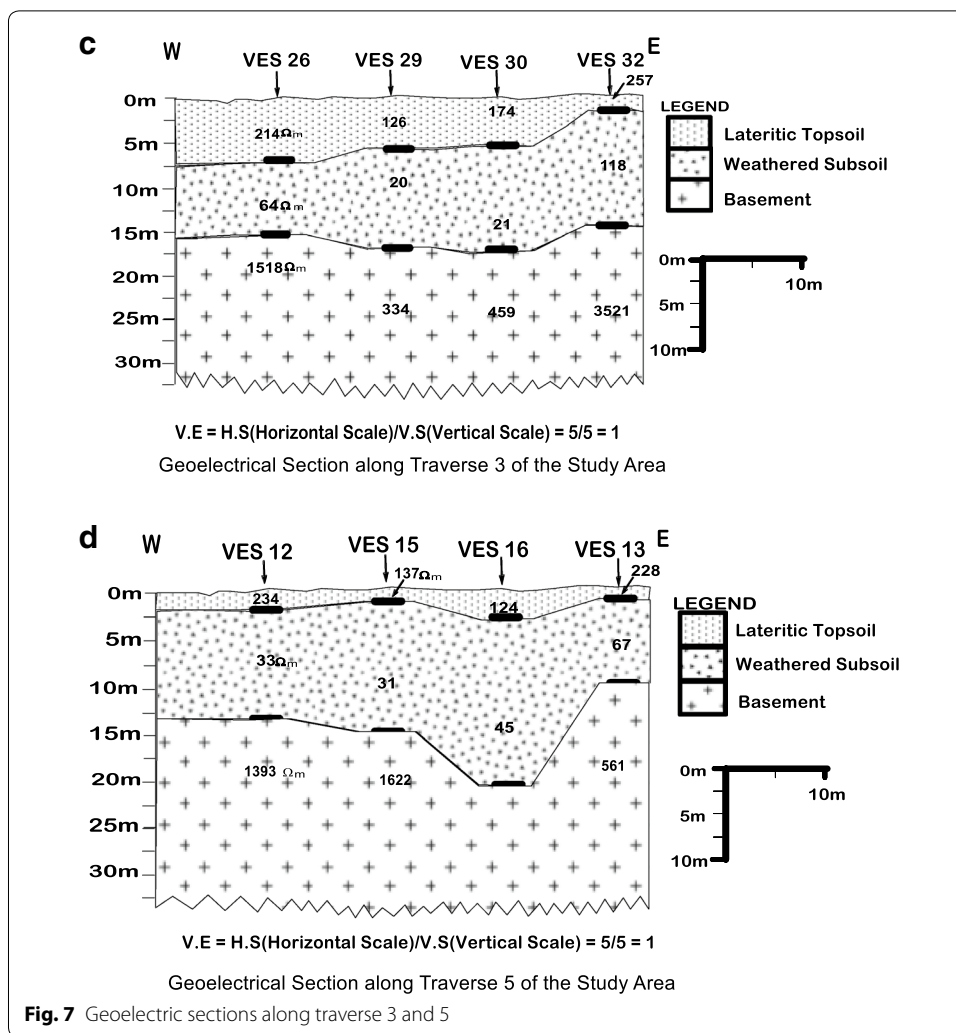
The isoresistivity map of the topsoil (Fig. 15) is diagnostic of fairly heterogeneous topsoil which is suggestive that it is composed of diverse types of earth materials. The isoresistivity map of the weathered layer reveals high apparent resistivity zones to fall around the central area with resistivity ranging between 1500 to 3600 Ωm. This zone is considered to be characteristic of lateritic to dry lateritic sand which is considered and classed as stable for civil engineering structures (Fig. 16).

GPR profiles (radagrams)

Eight representative GPR profiles are presented with Figs. 17, 18, 19, 20, 21 and 22 radar sections across the study area. The depth of penetration of the radar signals range from 20 to 22 m in the studied area. The GPR profiles show three distinct layers, with the upper layer having a thickness range of about 0.5–1 m and characterized by strong planar GPR reflections corresponding to lateritic topsoil. It is important to mention that the top layer however has high amplitude, parallel-even, uniform, continuous, alternating high and low reflection which stands out very conspicuous from the underlining layer which is hummocky with micro-scale diffraction. While directly below this is the weathered

Salako *et al. Geo-Engineering*   (2019) 10:11

Page 10 of 20
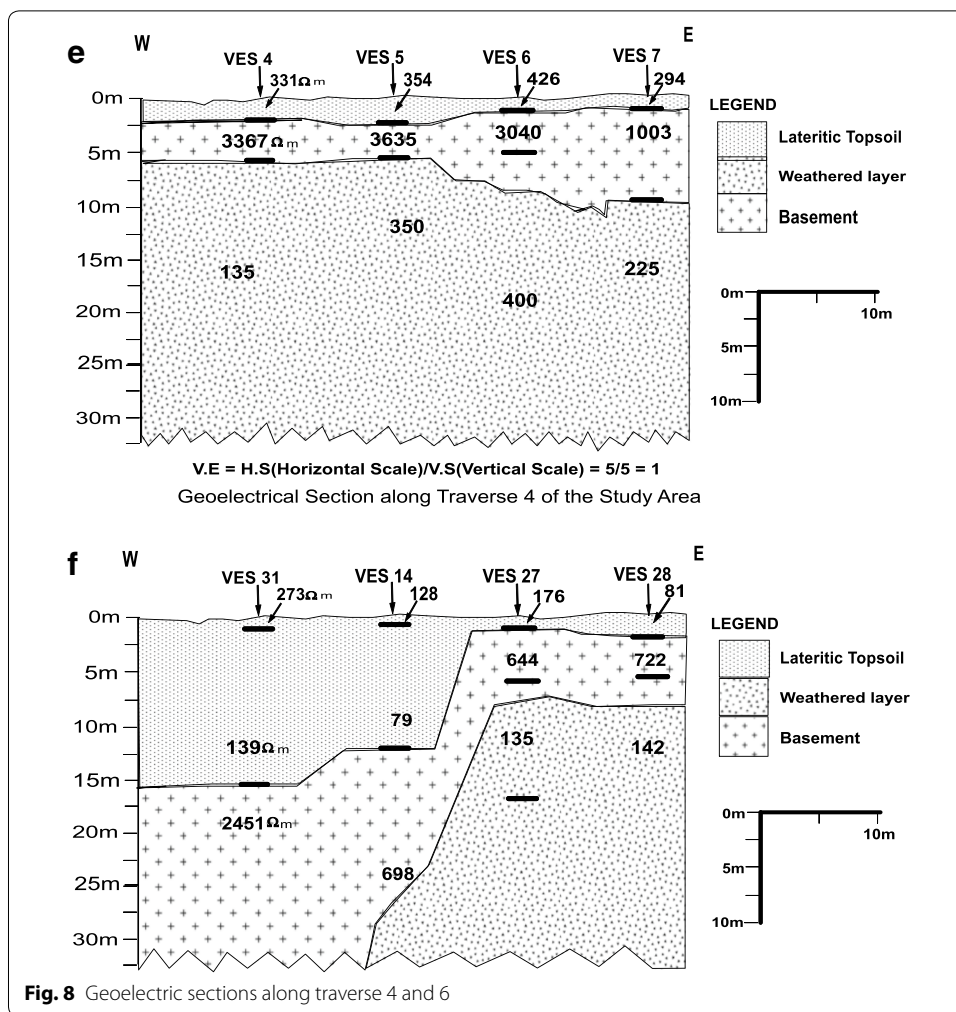
Fig. 8 Geoelectric sections along traverse 4 and 6

layer (clay with sand intercalations) characterized by smooth to nearly smooth, horizontal, chaotic, moderately continuous reflections with low amplitude extends from about 1–10.4 m. The last layer is the basement bedrock, with its top marked by strong reflective surface at depths of about 10.4 m, and extending to infinite thickness. The basement bedrock is characterized by chaotic reflection with micro-scale diffractions, this is probably due to its compact nature.

GPR Reflections in layer 2 (weathered layer) become weaker and less coherent with depth due to its relative higher moisture content within the layer. Linear, curvilinear and almost semi-inclined lineations are observed by the enclosed red box, yellow curves and green spheres (Figs. 17, 18, 19, 20, 21 and 22) but, most prominent in Figs. 17, 18, 19, 20, 21 and 22 where its effect is significant. The curvilinear structures in Figs. 18 and 19 most probably reflect buried pre-existing channels, that empties into the main drainage (Fig. 2). which were subsequently buried by depositional processes, acting as underground passage and conduits for subsurface water flow. The suspected channel is about 2.5–3 m in width. The structures enclosed in green circular sphere in Fig. 22 are probably seepage zones from fissures/fractures buried deep in the weathered layer/weathered/fractured basement. The fairly smooth reflections

Salako *et al. Geo-Engineering*   (2019) 10:11

Page 11 of 20

Fig. 9 Geoelectric sections along traverse 7 and 8
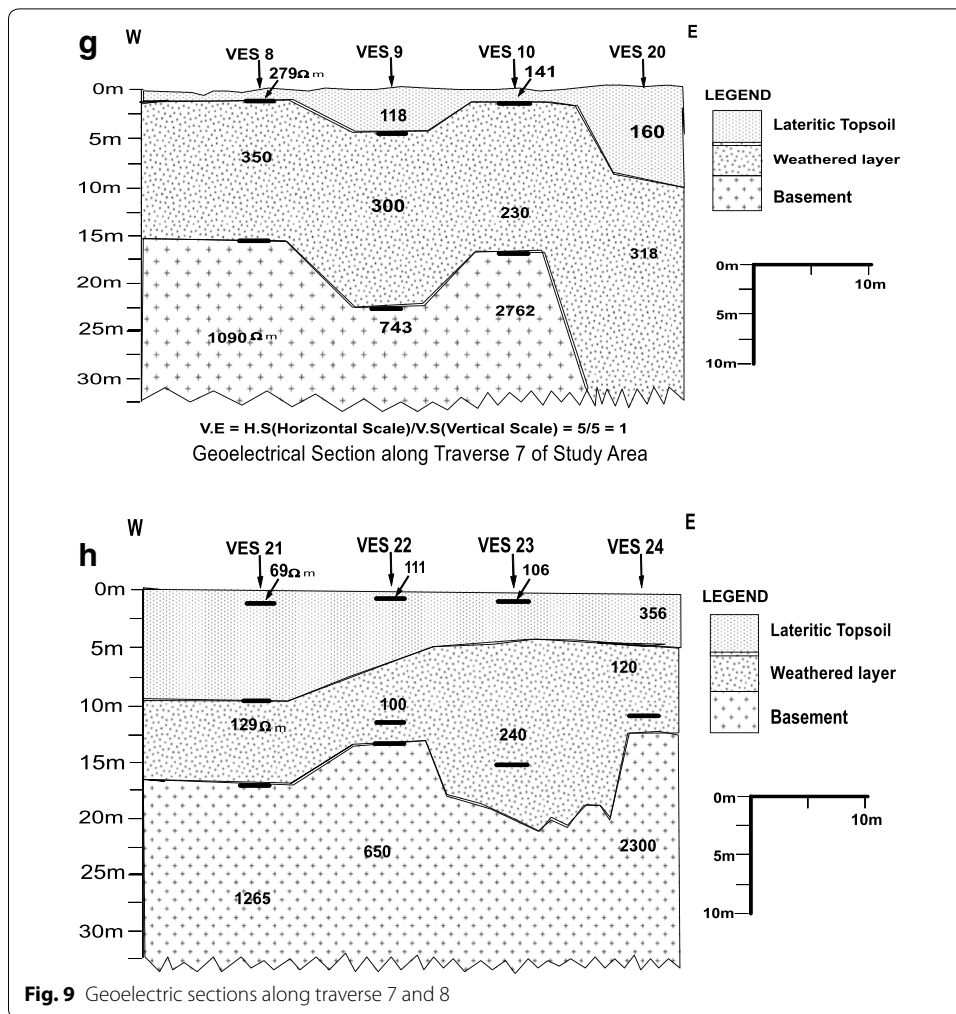
in Figs. 18, 19 and 21 may be due to water accumulations finding its way to the surface through fractures or fissures. The prominent presence of fractures and fissures in Figs. 17, 18, 20 and 22 with time is probably what results to a weakening of the soils' strength underneath the foundation of buildings in the investigated site.

Synthesis of results

Zones of high apparent resistivity coincide with thin overburden thickness and high basement relief/topography (Figs. 12, 13 and 14). This indicate a relatively thin thickness/shallow depth to a basement bedrock which is a far more competent layer as no known incompetent layer can underlay the infinitely continuous basement bedrock. The Geoelectric sections are overlaid on the radar sections (radagrams) as shown in Figs. 23, 24, 25, 26, 27 and 28. These are seen to show relatively fair correlation as the distinct lithologic layers on the geo-sections achieve a tie with the boundaries on the radar sections.
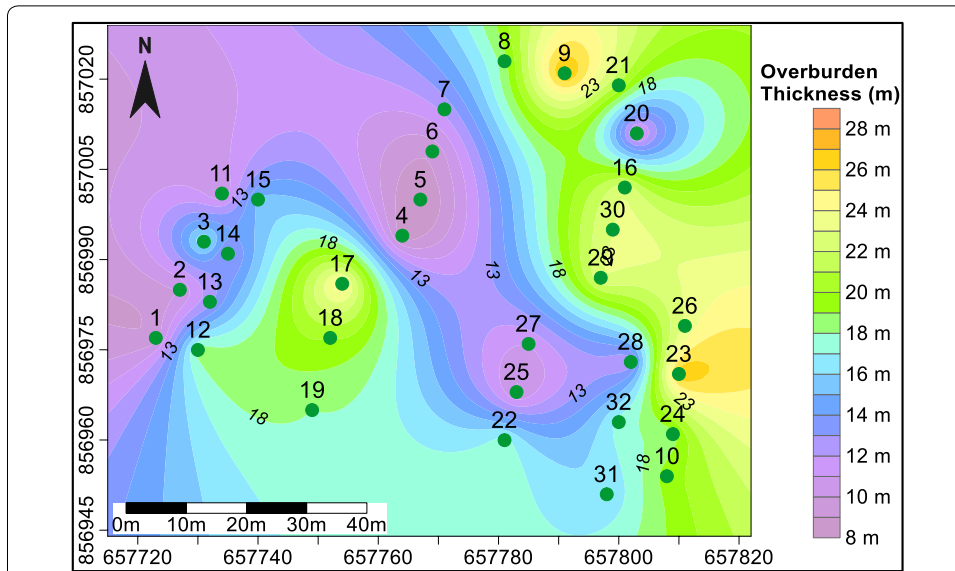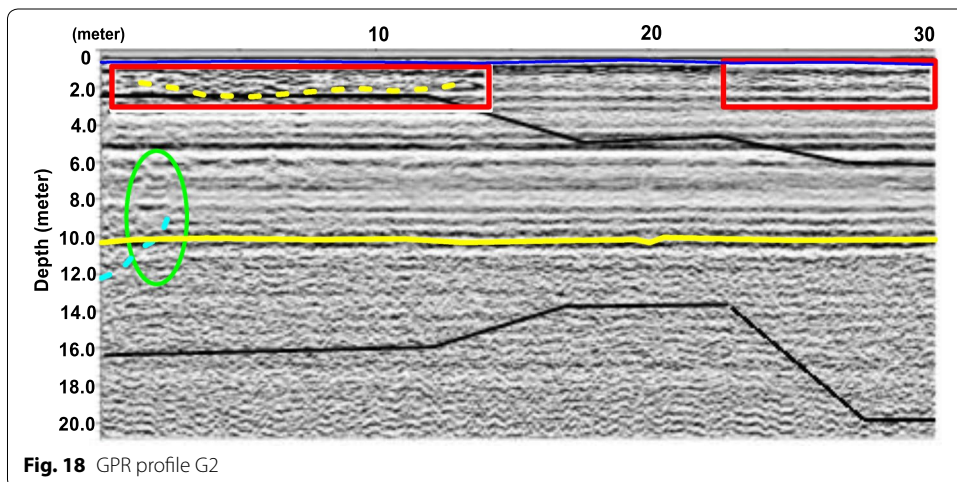
Fig. 10 Isopach map showing the topsoil thickness distribution

Fig. 11 Isopach map showing the weathered layer thickness distribution
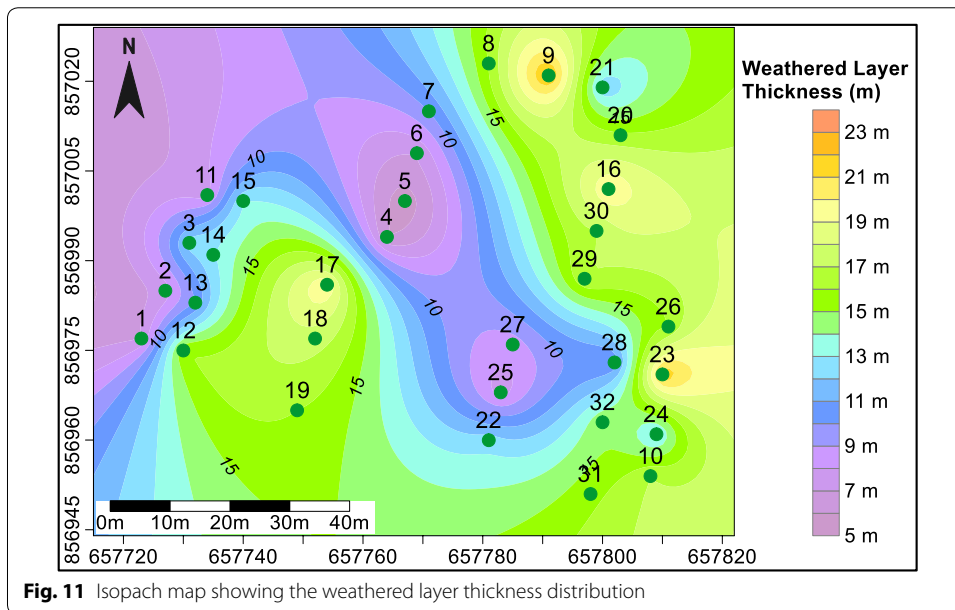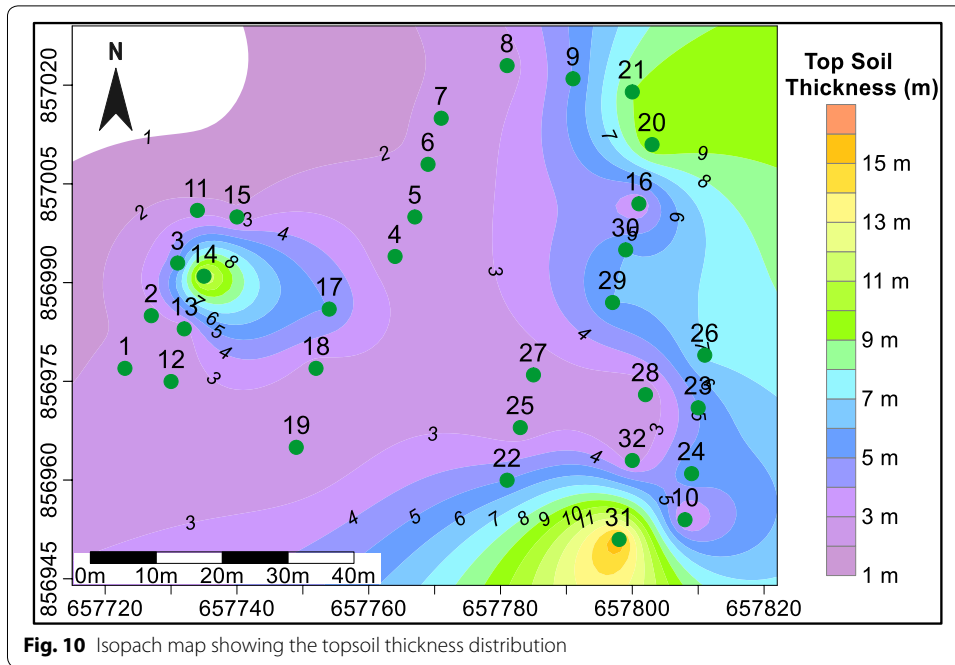
Discussions

From the Ground Penetrating Radar (GPR) survey, three clearly and distinct layers characterized by electromagnetic properties where delineated; with the uppermost layer (lateritic topsoil) having a thickness of about 2 m, the second layer (weathered layer) having a depth extension of about 6 m from the uppermost layer and the third layer (basement rock) forming the parent rock has an infinite extension. The weathered layer been the area of interest was found to be characterized smooth to nearly smooth reflections, with the presence of inclined features (probably fractures,

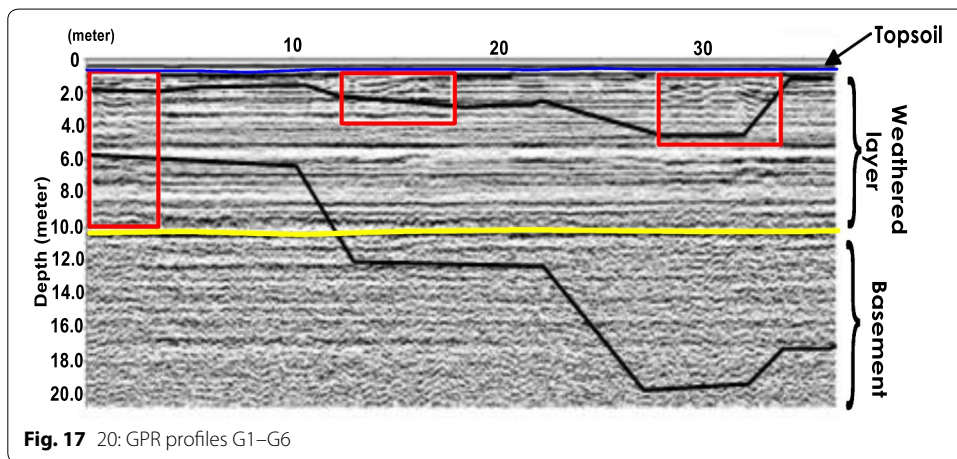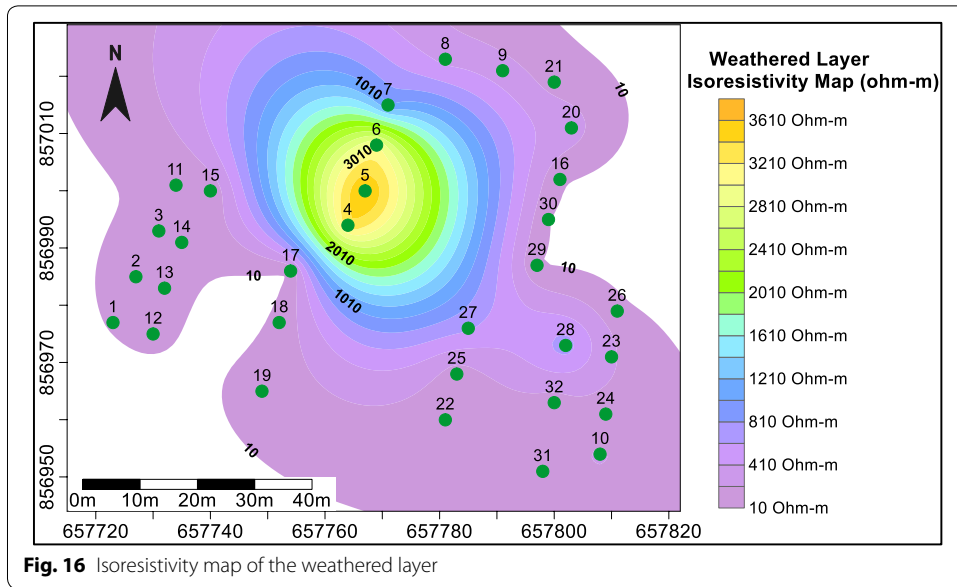**Fig. 12** Isopach map showing the overburden thickness distribution
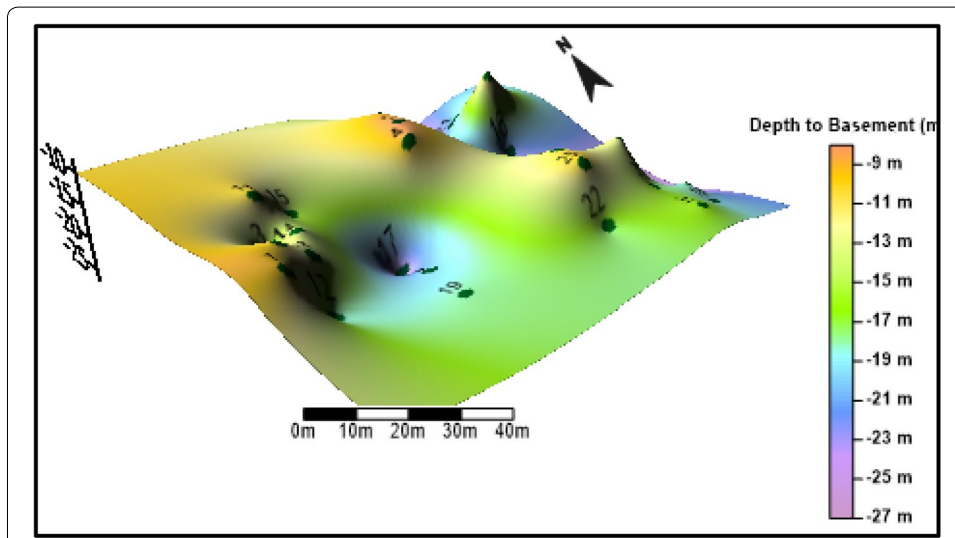
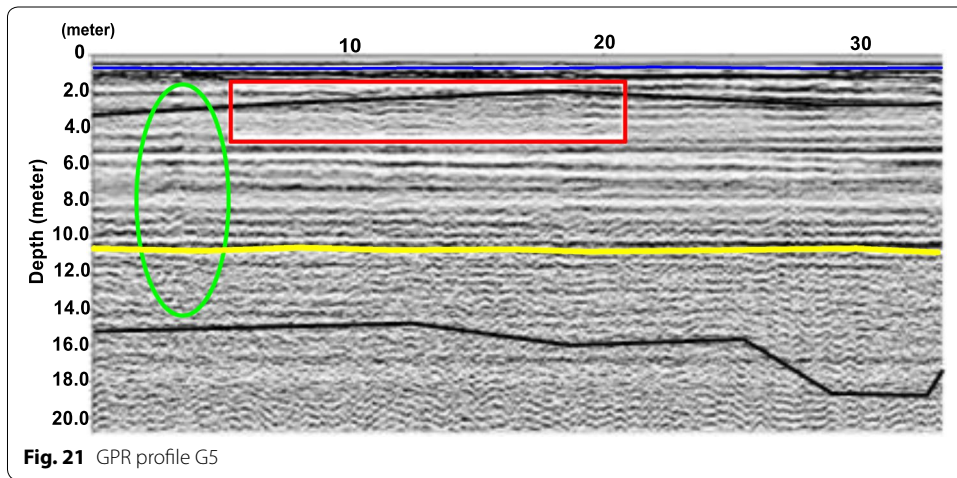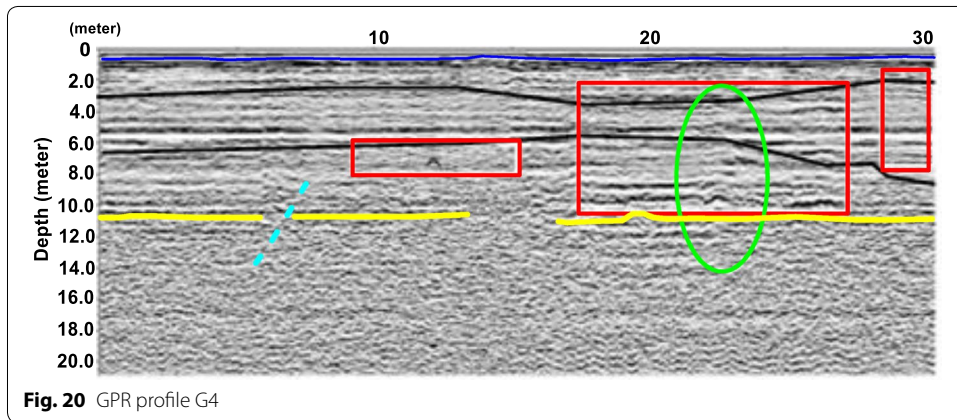**Fig. 13** Map showing basement topograhpy underlying the study site
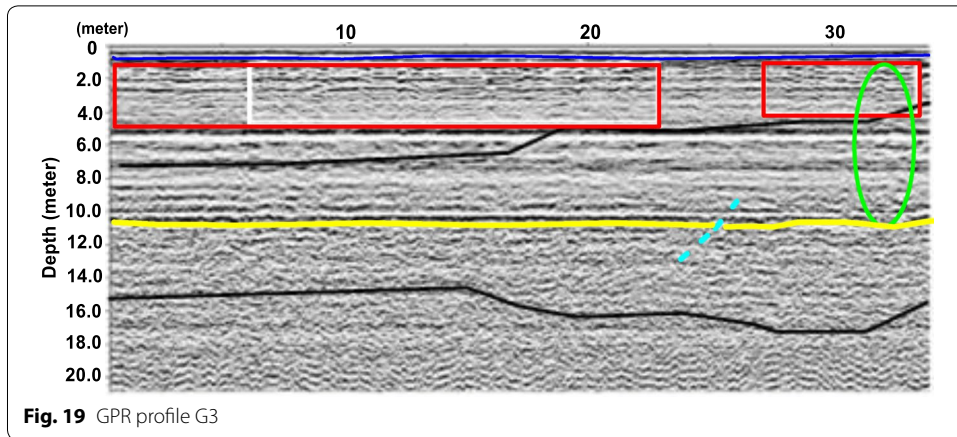
fissures) serving as pathways for water seeps unto the surface which gradually finds its way into some of the buildings through building cracks. The Electric Resistivity (ER) survey was found to complement the result of the GPR survey as it shows comparable soil conditions with varying subsurface layer resistivity. With particular interest is the weathered layer that shows anomalously low resistivity values ($< 65\ \Omega m$) probably indicative of presence of fractures, fissures through with groundwater thus seeps unto the surface. Also the anomalously low resistivity values could be attributed to the presence of clay and sand intercalations with the clay having the property of contraction and expansion thus resulting into cracks that groundwater could seep through thus gradually weakening the foundation. An integration of images obtained

Fig. 14 3D wireframe layer of basement relief underlying the area

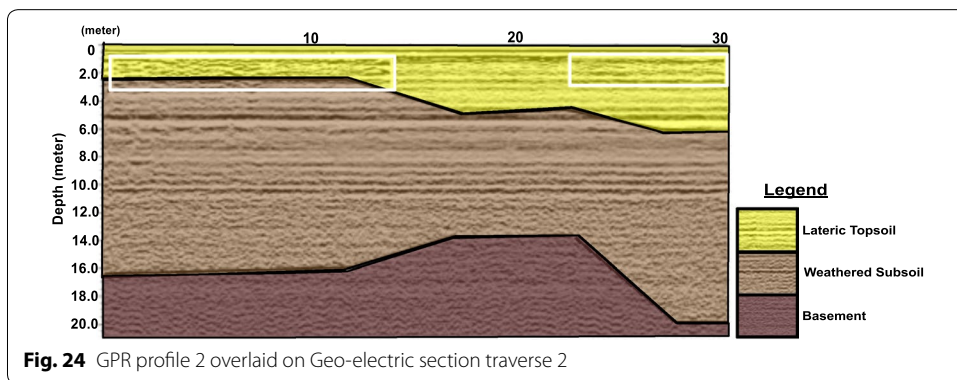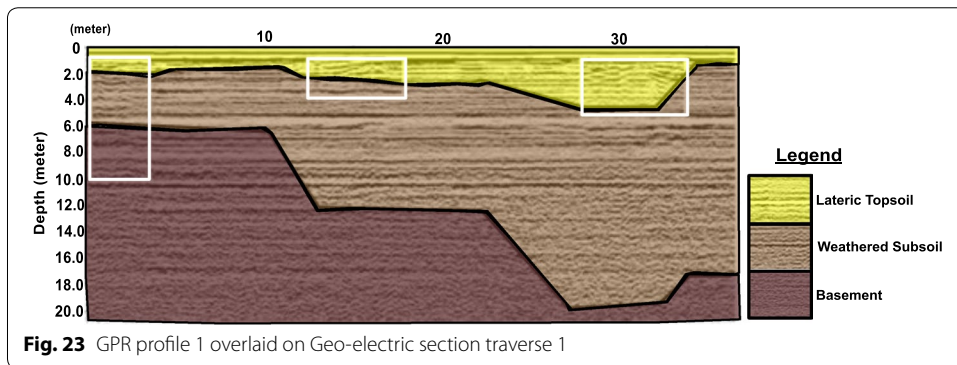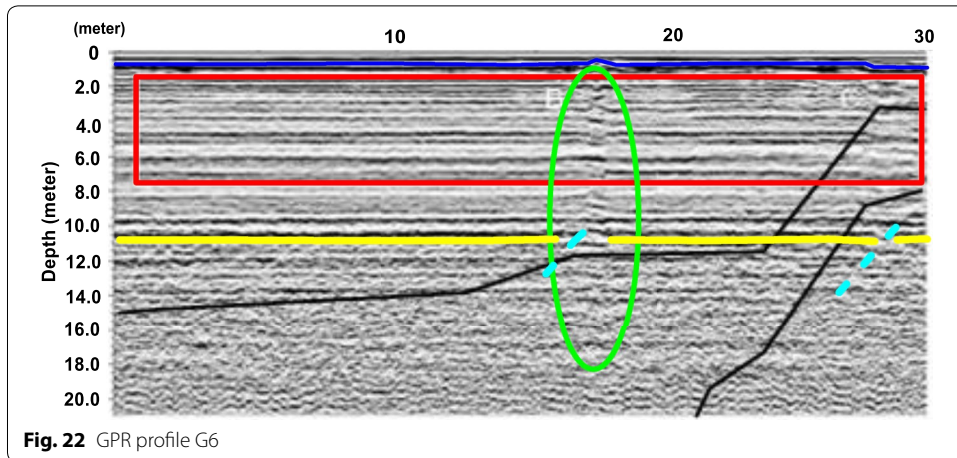**Fig. 15** Isoresistivity map of the topsoil
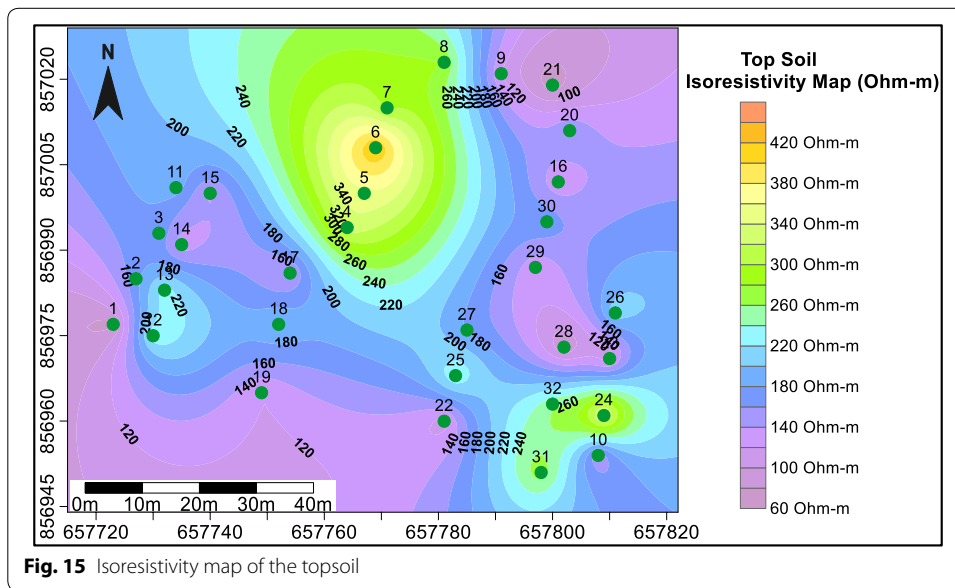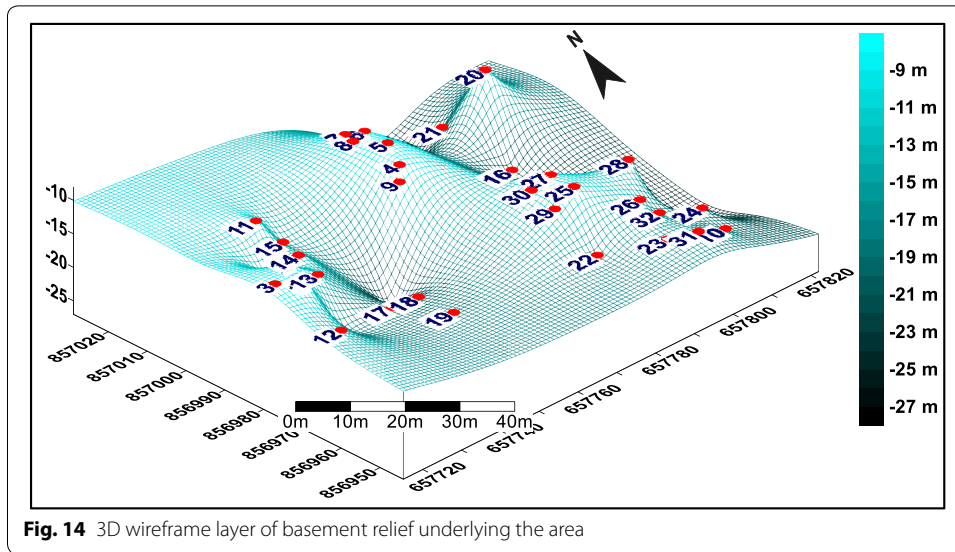
from the two surveys used showed that the dominance of clay material intercalated with sandstone and also the presence of fractures, fissures within the weathered layer is probably what leads to an instability of the building foundation in the study area.

Investigations performed in the study demonstrates that GPR response varies significantly with typical variations in rock/subsoil types cum porosity and soil saturation. Increasing water saturation in highly porous but less permeable clayey layers produced low reflection-coefficient values responsible for the smooth- near smooth GPR radar reflections in the clayey weathered layer sub-stratum. Hence, GPR response can be sensitive to subtle differences in rock properties and therefore can be a powerful tool for investigating subsurface heterogeneous soil properties. From the GPR

Salako *et al. Geo-Engineering*   (2019) 10:11

Page 15 of 20

Fig. 16 Isoresistivity map of the weathered layer

Fig. 17 20: GPR profiles G1–G6

Fig. 18 GPR profile G2

Fig. 19 GPR profile G3
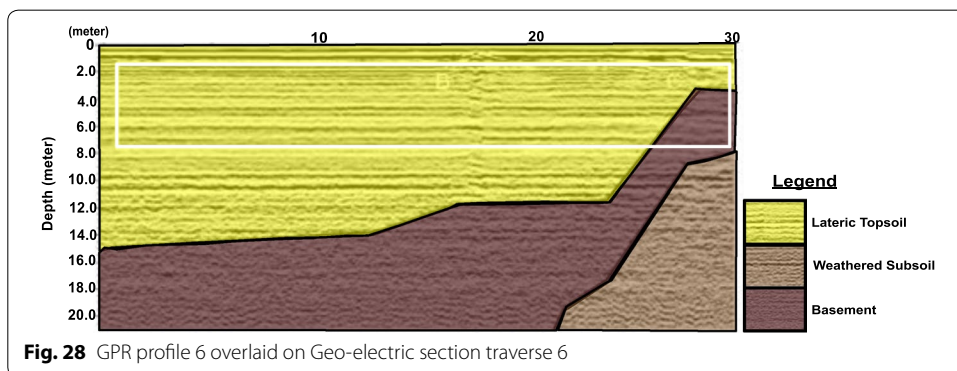

Fig. 20 GPR profile G4
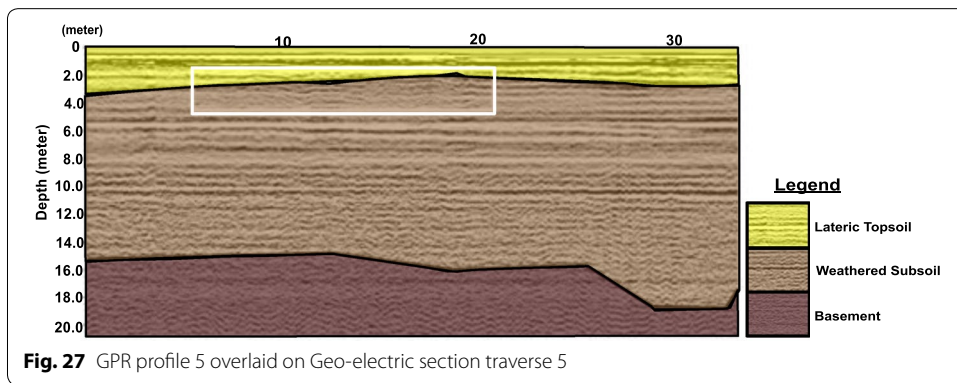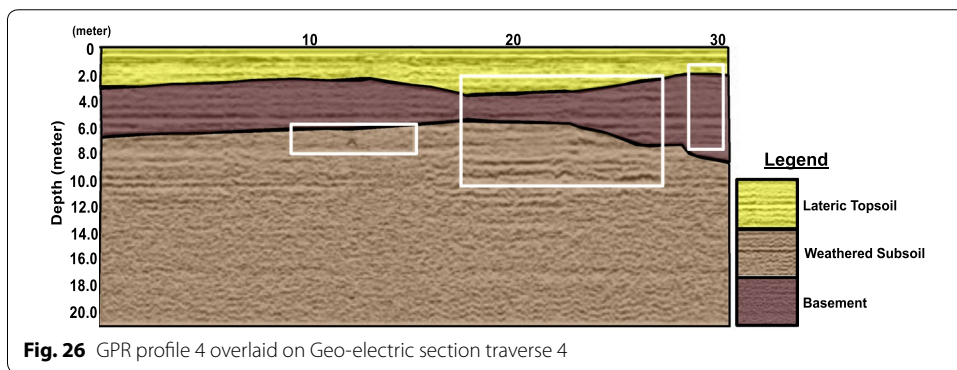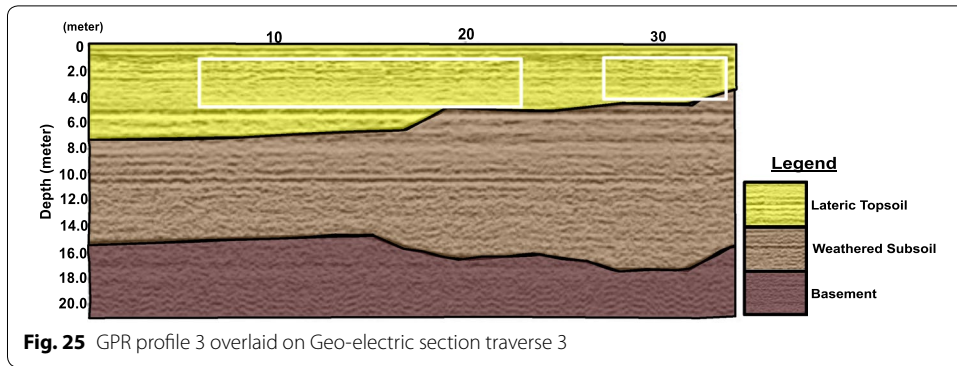

Fig. 21 GPR profile G5

radagrams (Figs. 17, 18, 19, 20, 21, 22), the reflection coefficient of the ground surface was increased by high water content in the underlying lithology (at about 0.8 m and 5.8 m), and the surface reflection are stronger compared to the surrounding area. This is also observed between the weathered layer and basement interface. Thus, the

Fig. 22 GPR profile G6

Fig. 23 GPR profile 1 overlaid on Geo-electric section traverse 1

Fig. 24 GPR profile 2 overlaid on Geo-electric section traverse 2

soil water content at the near-soil surface as described enhances the reflection. Thus, this exercise clearly demonstrated the capability of GPR to measure water-related soil properties, discriminate lithologies and geologic boundaries.

Conclusion and recommendation

From this study, distinct subsurface lithologies characterizing the study area were delineated using the electrical resistivity (ER) and the Ground Penetrating Radar (GPR) methods. These techniques were found very useful in delineating subsurface geologic features. The

Fig. 25 GPR profile 3 overlaid on Geo-electric section traverse 3

Fig. 26 GPR profile 4 overlaid on Geo-electric section traverse 4

Fig. 27 GPR profile 5 overlaid on Geo-electric section traverse 5

Fig. 28 GPR profile 6 overlaid on Geo-electric section traverse 6

GPR method integrated with the ER investigation of the study area further improved the quality of subsurface information by providing images with lateral continuity and vertical variations of the subsoil, reduction in the uncertainty of the interpretation, enhanced the precision with which subsurface structures such as fractures, faults and lineaments were mapped, and ambiguities in the interpretation were minimized. The integration of the two geophysical methods is an approach in carrying out geo-gnostic investigations at the study site, where invasive techniques, such as drillings, cannot be performed.

The results obtained established the existence of three (3) major lithologic/geologic layers consisting of top soil, weathered layer and the basement. The processed GPR radagram datasets were able to probe to about 22 m. The materials are made up of the topsoil (lateritic), weathered layers (saturated clay), and basement rocks. The combined investigation shows that the second lithological (weathered) layer consists of clayey materials (with characteristic low layer resistivity ($< 100\ \Omega m$), which are potential zones for groundwater accumulation, having the tendency of absorbing water as a result of intense fractures, hence may exhibit high swelling potential and collapse under imposed load stress. This is obvious from the walls of some civil structures in the neighborhood of the study area which are wet, and some cracked. From the integrated engineering geophysical site investigation undertaken in the study area, it can be inferred that the possible causes of the seepage, leading to building failure in the studied area, are near-surface linear (geological) features such as micro fractures, lithological contacts beneath the area, and buried channels. These features act as zones of weaknesses and pathways that serves as conduits for the ingression and accumulation of water, and hence leading to some portions of failure in civil structures in the study area. This study has revealed that this was due to siting the foundation on lithologic materials that have differentially settled, and or subsurface structures that act as groundwater conduits.

Therefore, it is recommended that construction of superstructures or foundation with continuous footing therefore requires an engineering intervention such as pilling to a depth of about 10–14 m. Also, injection of expansive polyurethane resin can be used to remediate differential settlement issues, whereby the resin is injected incrementally under a structure to achieve a desired foundation level, forming a composite resin–clay material [2, 24]. But, this should be applied cautiously after further geotechnical investigation. Removal of unstable subbase soil materials to layers to better integrity can also be done, and replaced with more stable earth materials before the commencement of civil works.

Authors' contributions
AOS, AAA conceived the idea for the research work while AGO gave additional and valuable inputs in the interpretation and presentation of dataset and results. AOS took the lead in writing the manuscript. All authors read and approved the final manuscript.

References

1. Akinrinade JO, Adesina RB (2016) Hydrogeophysical investigation of groundwater potential and aquifer vulnerability prediction in basement complex terrain—a case study from Akure. De Gruyter Open, Southwestern Nigeria. https://doi.org/10.1515/rmzmag-2016-0005
2. Buzzi O, Fityus S, Sloan SW (2010) Use of expanding polyurethane resin to remediate expansive soil foundations. Can Geotech J 47:623–634
3. Conyers LB, Goodman D (1997) Ground Penetrating Radar for Archaeology. Walnut Creek, California
4. Cosenza P, Marmet E, Rejiba F, Jun Cui Y, Tabbagh A, Charlery Y (2006) Correlations between geotechnical and electrical data: a case study at Garchy in France. J Appl Geophys 60:165–178
5. Davis JL, Annan AP (1989) Ground penetrating radar for high resolution mapping of soil and rock stratigraphy. Geophys Prospect 37(5):531–551
6. Forte E, Dossi M, Pipan M, Colucci RR (2014) Velocity analysis from common offset GPR data inversion: theory and application to synthetic and real data. Geophys J Int 2014(197):1471–1483. https://doi.org/10.1093/gji/ggu103
7. Freeland RS, Odhiambo LO (2007) Subsurface characterization using textural features extracted from GPR data. Trans ASABE 50(1):287–293
8. Giannakis I, Giannopoulos A, Warren C (2016) A realistic FDTD numerical modeling framework of ground penetrating radar for landmine detection. IEEE J Sel Top Appl Earth Observations Rem Sens 9(1):1–15
9. Godio A, Strobbia C, De Bacco G (2006) Geophysical characterization of a rockslide in an alpine region. Eng Geol 83:273–286
10. Gonzalez-Huici, M. A. 2012. A strategy for landmine detection and recognition using simulated GPR responses. In: Proceedings 14th Conference on Ground Penetrating Radar, Shanghai
11. Juanah ME, Ibrahim S, Sulaiman W, Latif P (2012) Groundwater resources assessment using integrated geophysical techniques in the southwestern region of Peninsular Malaysia. Arab J Geosci 1:1–16
12. Kazunori T, Jan I, Holger P, Seiichiro K (2012) Basics and application of ground penetrating radar as a tool for monitoring irrigation process, problems, perspectives and challenges of agricultural water management, Dr. Manish Kumar (Ed.), ISBN: 978-953-51-0117-8, InTech
13. Khatri R, Shrivastava VK, Chandak R (2011) Correlation between vertical electric sounding and conventional methods of geotechnical site investigation. Int J Adv Eng Sci Technol 4:042–053
14. Liu C, Evett JB (2008) Soils and foundation. Pearson International, Singapore
15. Mallent D, Toride N, Tseng P-H (1997) Numerical simulation of chemical transport in a physically heterogeneous soil profile. In: International conference on contaminated sediments, Rotterdam, The Netherlands, 7–11 September
16. McLean AC, Gribble LO (1979) Geology for engineers. George Allen & Unwin
17. Moysey S, Knight RJ, Jol HM (2006) Texture-based classification of ground penetrating radar images. Geophysics, Vol. 71, No. 6 (November–December 2006); P. K111–K118, 9 Figs. https://doi.org/10.1190/1.2356114
18. Neal A (2004) Ground-penetrating radar and its use in sedimentology: principles, problems and progress. Earth-Sci Rev 66:261–330
19. Obaje NG (2009) Geology and mineral resources of nigeria. Springer, New York, p 117
20. Onishi K, Rokugawa S, Katoh Y (2004) Estimation of saline regions using ground penetrating radar. In: Proceeding of 10th international conference on ground penetrating radar, Delft, The Netherlands, 21–24 June 2004, pp 509–512
21. Owen R, Gwavava O, Gwaze P (2006) Multi-electrode resistivity survey for groundwater exploration in the Harare greenstone belt, Zimbabwe. Hydrogeol J 14:244–252
22. Oyinloye, A. O. 2011. Geology and Geotectonic Setting of the Basement Complex Rocks in South Western Nigeria: Implications on Provenance and Evolution, Earth and Environmental Sciences, Dr. Imran Ahmad Dar (Ed.), ISBN: 978-953-307-468-9, InTech, http://www.intechopen.com/books/earthand-environmental-sciences/geology-and-geotectonic-setting-of-the-basement-complex-rocks-in-southwestern-nigeria-implications
23. Ozegin KO, Adetoyinbo AA, Jegede SI, Ogunseye TT (2016) Troubled roads: application of surface geophysics to highway failures of the sedimentary terrain (Iruekpen-Ifon Road) of Edo State, Nigeria. Acad J Int J Phys Sci 11(22):296–305. https://doi.org/10.5897/IJPS2016.4546
24. SikaFix construction manual, 2015. Waterproofing ground consolidation, stabilization and waterstopping in tunneling & mining. SIKA SERVICES AG, Zürich, Switzerland. http://www.sika.com
25. Tijani M, Crane E, Upton K, Dochartaigh BÉ, Bellwood-Howard I (2018) Africa groundwater atlas: hydrogeology of Nigeria. British Geological Survey. http://earthwise.bgs.ac.uk/index.php/Hydrogeology_of_Nigeria. Accessed 5 July 2019
26. Tosti F, Benedetto A (2012) Pavement pumping prediction using ground penetrating radar. Procedia Soc Beh Sci 53:1045–1054. https://doi.org/10.1016/j.sbspro.2012.09.954
27. van den Bosch I (2006) Accurate modelling of ground penetrating radar for detection and signature extracting of mine-like targets buried in stratified media. Ph.D. thesis, University Catholique de Louvain and Royal Military Academy, Belgium
28. Vander Velpen BPA (2004) WIN RESIST™: An Electrical resistivity inversion program
29. Warren C, Giannopoulos A (2016) Characterisation of a ground penetrating radar antenna in lossless homogeneous and lossy heterogeneous environments. Sign Process 132:221–226. https://doi.org/10.1016/j.sigpro.2016.04.010
30. Warren C, Giannopoulos A, Giannakis I (2016) gprMax: open source software to simulate electromagnetic wave propagation for Ground Penetrating Radar. Comput Phys Commun 209:163–170. https://doi.org/10.1016/j.cpc.2016.08.020
31. Yusuf GA, Akinrinade OJ, Ojo JS (2015) An engineering site characterization using geophysical methods: a case study from Akure, southwestern Nigeria. J Earth Sci Geotech Eng 5(4):57–77

Publisher's Note

Springer Nature remains neutral with regard to jurisdictional claims in published maps and institutional affiliations.